https://doi.org/10.5194/esd-2019-83
Preprint. Discussion started: 16 January 2020

Earth System Dynamics
Discussions
Open Access
EGU

Climate-groundwater dynamics inferred from GRACE and the role of hydraulic memory

Simon Opie[1,*], Richard G. Taylor[1], Chris M. Brierley[1], Mohammad Shamsudduha[2] and Mark O. Cuthbert[3,4]

[1] Department of Geography, University College London, London, UK
[2] Department of Geography, University of Sussex, Falmer, Brighton, UK
[3] School of Earth and Ocean Sciences, Cardiff University, Cardiff, UK
[4] Connected Waters Initiative Research Centre, University of New South Wales, Sydney, New South Wales, Australia
[*] Corresponding author: Simon Opie (simon.opie.18@ucl.ac.uk)

Abstract

Groundwater is the largest store of freshwater on Earth after the cryosphere and provides a substantial proportion of the water used for domestic, irrigation and industrial purposes. Knowledge of this essential resource remains incomplete, in part, because of observational challenges of scale and accessibility. Here we examine a 14-year period (2002-2016) of GRACE observations to investigate climate-groundwater dynamics of 14 tropical and sub-tropical aquifers selected from WHYMAP's 37 large aquifer systems of the world. GRACE-derived changes in groundwater storage resolved using GRACE JPL Mascons and the CLM Land Surface Model are related to precipitation time series and regional-scale hydrogeology. We show that aquifers in dryland environments exhibit long-term hydraulic memory through a strong correlation between groundwater storage changes and annual precipitation anomalies integrated over the time series; aquifers in humid environments show short-term memory through strong correlation with monthly precipitation. This classification is consistent with estimates of Groundwater Response Times calculated from the hydrogeological properties of each system, with long (short) hydraulic memory associated with slow (rapid) response times. The results suggest that groundwater systems in dryland environments may be less sensitive to seasonal climate variability but vulnerable to long-term trends from which they will be slow to recover. In contrast, aquifers in humid regions may be more sensitive to seasonal climate disturbances such as ENSO-related drought but may also be relatively quick to recover. Exceptions to this general pattern are traced to human interventions through groundwater abstraction. Hydraulic memory is an important factor in the management of groundwater resources, particularly under climate change.

https://doi.org/10.5194/esd-2019-83
Preprint. Discussion started: 16 January 2020

Earth System Dynamics Discussions

1.0. Introduction:

The availability of freshwater is essential for sustaining human life, economic security, and access to the benefits of a wide range of ecosystem services (Taylor et al., 2013a). After the cryosphere, groundwater is the second largest store of freshwater on the planet supplying 36% of domestic water, 42% of irrigation for agriculture and 27% of industrial water use (Döll et al., 2012). Baseflow from groundwater sustains rivers and wetlands in the absence of rainfall and is therefore fundamentally important to the ecology of semi-arid and arid regions in particular (Alley et al., 2002; Graaf et al., 2019). Future climate change in which anthropogenic emissions of greenhouse gases transform patterns of natural variability, together with substantial socio-economic change, predicate that management of freshwater resources will become a critical task (Famiglietti, 2014). In a climate where it is broadly predicted that 'wet gets wetter, dry gets drier' (Trenberth, 2011), water storage at and below the land surface will be a vital tool in enabling successful adaptation to the changing global environment (Damkjaer and Taylor, 2017; Wada, 2016).

Despite the importance of groundwater there are considerable gaps in current knowledge and understanding (Güntner et al., 2007). Direct observations of groundwater are sparse in relation to its geographical scale so most global or regional groundwater data are based on output from large-scale models. These include global hydrological models (GHMs) (Sood and Smakhtin, 2015) or land- surface models (LSMs) (Bierkens, 2015; Overgaard et al., 2006; Wood et al., 2011) for which there are often insufficient data available to constrain or calibrate (Döll et al., 2016). Model simulation of key processes such as soil hydrodynamics and groundwater recharge is therefore based on theoretical frameworks rather than field data (Scanlon et al., 2002). As a result, there is also considerable uncertainty about climate-groundwater dynamics. Recent work in this area has either focused on localised observations of changes in Groundwater Storage (ΔGWS) from piezometry (Cuthbert et al., 2019b) or occurred adjacent to large centres of population where human intervention, through extraction of groundwater by pumping, can greatly influence observational measurements (Scanlon et al., 2018). In the context of a recent, rapid escalation in groundwater abstraction of ~15% per decade from 1960 to 2010 (Wada et al., 2014), an understanding of climate-groundwater dynamics, supported by large-scale observational data, is required to inform sustainable access to groundwater resources (Taylor et al., 2009).

In response to the lack of in situ field observations, remote-sensing by satellite is increasingly being utilised to expand the scope of observational data available to Earth sciences (Acker and Leptoukh, 2007). An important advance in the quality of global data for hydrological studies has come from the Gravity Recovery and Climate Experiment (GRACE), a collaboration

https://doi.org/10.5194/esd-2019-83
Preprint. Discussion started: 16 January 2020


Earth System Dynamics Discussions

between the National Aeronautics and Space Administration (NASA) in the USA and the German Aerospace Centre (DLR) launched in March 2002 (Tapley et al., 2004). Completed sets of ~monthly measurements are used to derive the changes in mass at the Earth's surface and from these data mass fluxes can be extracted that directly relate to the hydrosphere. Over land, the flux is expressed as a change in Total Water Storage (ΔTWS) at a spatial resolution of ~300km and with an expected accuracy of better than 2 cm equivalent water height (EWH) (Tapley et al., 2004). GRACE ceased operation due to battery failure in mid-2016 having created a record of 163 monthly gravity solutions (Tapley et al., 2019). Although GRACE operated for ten years longer than anticipated at its launch, it is a relatively brief dataset in relation to large-scale climate patterns impacting the global hydrological system with frequencies of several years or decades (e.g. Pacific Decadal Oscillation (PDO), Atlantic Multidecadal Oscillation (AMO)). Nevertheless, inter-annual periodicities associated with the El Niño Southern Oscillation (ENSO) and the Antarctic Circumpolar Wave (ACW) have been detected (Mémin et al., 2015; Ni et al., 2018; Phillips et al., 2012).

Intrinsic parameters of GRACE data effectively define the spatial and temporal dimensions of this study but there are additional constraints related to the derivation of ΔGWS data from GRACE ΔTWS that also need to be considered. The sub-division of GRACE ΔTWS into its component parts, including ΔGWS, requires the application of GHM or LSM output that is itself subject to associated uncertainty, as already noted (Döll et al., 2014). It has been demonstrated that there is relatively poor correlation between GRACE and GHMs/LSMs in the evaluation of ΔTWS, with significant discrepancies at the basic level of whether storage trends are increasing or decreasing (Scanlon et al., 2018). These findings have been confirmed with reference to regional piezometric groundwater measurements from tropical aquifers in Africa (Bonsor et al., 2018). Thus, the application of GRACE data to ΔGWS implies three distinct areas of uncertainty: in the processing of the GRACE signal, accuracy of GHM/LSM model projections and mutual consistency of the observed (GRACE) and modelled (GHM/LSM) data (Long et al., 2015).

This study investigates the spatio-temporal properties of climate-groundwater dynamics using a subset of the 37 Large Aquifer Systems of the World (LASW) as defined by the Worldwide Hydrogeological Mapping and Assessment Programme (WHYMAP) ("BGR - WHYMAP - Large Aquifers," 2008), and shown in **Figure S1**. This subset comprises aquifers that lie broadly within the tropics and sub-tropics climate variability is mostly defined by rainfall (Shepherd, 2014). The 14 aquifers selected are listed in **Table 1** together with their key characteristics including Aridity Index (AI) calculated from the Consultative Group for International Agriculture Research's Consortium for Spatial Information (CGIAR-CSI) Global-Aridity Dataset (Trabucco and Zomer, 2019), shown in **Figure 1**. Following the work of (Shamsudduha and Taylor, 2019), the groundwater storage response to

https://doi.org/10.5194/esd-2019-83
Preprint. Discussion started: 16 January 2020

Earth System Dynamics
Discussions
Open Access
EGU

regional climate variability for these 14 large scale aquifer systems is investigated using ΔGWS data extracted from the whole of the available GRACE ΔTWS time series (August 2002 – July 2016) together with climate data that are defined by the areal extent of each of the aquifer systems.

Several studies have used GRACE data to examine storage changes within a particular GW system e.g. (Becker et al., 2010; Bonsor et al., 2018; Chen et al., 2016, 2010; Henry et al., 2011; Z. Huang et al., 2015; Ramillien et al., 2014; Shamsudduha et al., 2017, 2012; Tiwari et al., 2009; Xavier et al., 2010; Yeh et al., 2006). Here, we examine the dynamics of climate-groundwater interactions inferred from the underlying patterns of large-scale ΔGWS in response to extremes of precipitation. We find that hydraulic memory (HM) is a key component in the classification of groundwater responses to climate variability. We then seek to reconcile the results with reference to the physical characteristics of individual aquifer systems (Cuthbert et al., 2019a) whilst accounting for anomalous responses in ΔGWS to climate variability.

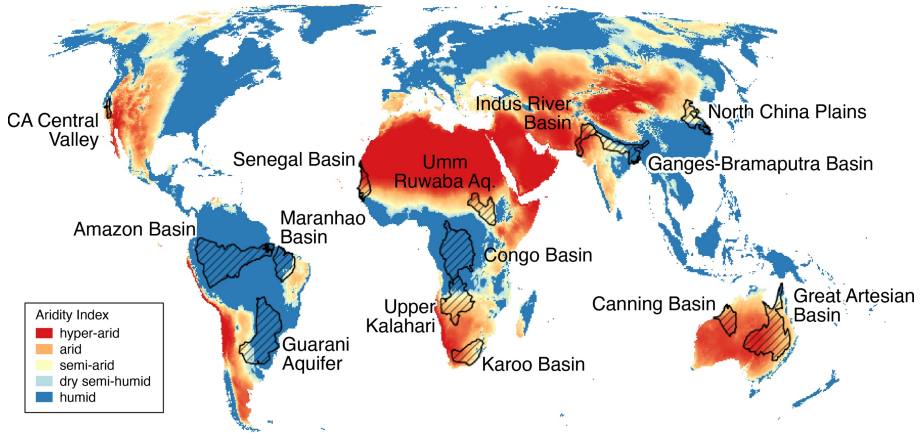

Figure 1: 14 of the World's Large-scale Aquifers (the Study Aquifers) overlaid on CGIAR-CSI Global-Aridity dataset *(Trabucco & Zomer, 2019).*

https://doi.org/10.5194/esd-2019-83
Preprint. Discussion started: 16 January 2020

Earth System Dynamics
Discussions
Open Access
EGU

WHYMAP Aquifer Number	Aquifer name	Continent	Population (millions)	Aquifer area (km^2)	Proportion of Irrigation GW fed (%)	Climate zone based on aridity index	Mean (2002-16) annual precipitation (mm)	Rainfall variability (%)
5	Senegal-Mauritanian Basin	Africa	17.77	295k	1.0	Semi-Arid	540	14.6
8	Umm Ruwaba Aquifer	Africa	10.52	509k	0.0	Semi-Arid	789	10.7
10	Congo Basin	Africa	34.74	1.49m	0.0	Humid	1566	5.6
11	Upper Kalahari-Cavelai-Zambezi Basin	Africa	6.02	1.00m	0.1	Semi-Arid	819	10.0
13	Karoo Basin	Africa	14.53	568k	2.1	Semi-Arid	479	17.6
16	California Central Valley Aquifer System	North America	8.10	71k	57.8	Semi-Arid	515	32.0
19	Amazon Basin	South America	8.93	2.28m	1.0	Humid	2505	8.3
20	Maranhao Basin	South America	10.81	593k	32.6	Humid	1502	15.7
21	Guarani Aquifer (Parana Basin)	South America	47.84	1.83m	20.5	Humid	1450	10.6
23	Indus River Basin	Asia	155.85	308k	31.0	Arid	375	16.2
24	Ganges-Brahmaputra Basin	Asia	596.44	616k	55.8	Humid	1391	12.1
29	North China Plains Aquifer System	Asia	336.70	439k	37.1	Dry Sub-Humid	826	10.0
36	Great Artesian Basin	Australia	0.20	1.77m	0.9	Arid	444	28.9
37	Canning Basin	Australia	0.01	433k	0.4	Arid	443	21.2

Table 1: Characteristics of the 14 Aquifer Systems selected for the study according to the WHYMAP and CGIAR-CSI databases with statistics giving (L to R): total number of resident population, aquifer area, proportion of irrigation GW-fed, mean aridity index classification (Trabucco and Zomer, 2019), mean annual rainfall and mean variability in annual rainfall.

https://doi.org/10.5194/esd-2019-83
Preprint. Discussion started: 16 January 2020

Earth System Dynamics Discussions

Methods:

2.1. *GWS derived from GRACE data:*

Mass fluxes relating to the hydrosphere contained in the GRACE land-signal measurement of changes in the Earth's gravitational field are defined as ΔTWS. In order to obtain information relating specifically to groundwater, this signal is separated into the component parts that comprise TWS, generally represented as:

$$\Delta TWS = \Delta GWS + \Delta SWS + \Delta SMS + \Delta SNS \quad (1)$$

where SWS is surface water storage, SMS is soil moisture storage and SNS is snow-water equivalent storage. ΔGWS is then derived from ΔTWS according to the following equation:

$$\Delta GWS = \Delta TWS - (\Delta SWS + \Delta SMS + \Delta SNS) \quad (2)$$

The locations of the 14 aquifers are outside areas where changes in snow-water equivalent substantially impact ΔTWS (Getirana et al., 2017). ΔSNS can consequently be omitted so that Eq. (2) can be rewritten for the purposes of this particular study as:

$$\Delta GWS = \Delta TWS - (\Delta SWS+\Delta SMS) \quad (3)$$

Since GRACE started transmitting, several solutions have been developed for analysing and producing GRACE ΔTWS data to increasing levels of accuracy, with the intention that the data be readily and freely available for research (Landerer and Swenson, 2012). In this instance, three different products were drawn from Shamsudduha and Taylor (2019), two of which are spherical harmonics (SH) solutions comprising CSR Land (version RL05.DSTvSCS1409) from the Jet Propulsion Laboratory (JPL) at NASA and CNES/GRGS (version RL03-v1) from the French Centre National d'Etudes Spatiales, and one JPL-Mascon (version RL05M 1.MSCNv01) from JPL-NASA. To derive ΔTWS, all GRACE solutions require additional processing that include corrections for glacial isostatic rebound and atmospheric mass variation (Landerer and Swenson, 2012). SH solutions also require spatial filtering (or 'de-striping') whereas JPL-Mascon does not as it directly converts the GRACE

https://doi.org/10.5194/esd-2019-83
Preprint. Discussion started: 16 January 2020


Earth System Dynamics Discussions Open Access EGU

signal into mass concentration blocks (Mascons), rendering monthly gravitational fields directly as 3ºx3º gridded spatial components to reduce errors (Watkins et al., 2015).

On inspection, the divergence between the 3 ΔTWS datasets was significant when summed over the time series. The relatively large coefficient of variance (COV), -104%, calls into question use of an ensemble mean for this study. Such an approach may be appropriate for the use of SH products alone (Sakumura et al., 2014) but it is preferable not to combine SH products and Mascons (Landerer, pers. comm.). Consequently we rely solely on the JPL-Mascon dataset possessing a better signal-to-noise ratio and potentially less error (Scanlon et al., 2016; Watkins et al., 2015; Xie et al., 2018). The employed JPL-Mascon dataset has been spatially sampled at a 0.5º grid using dimensionless scaling factors provided as 0.5ºx0.5º bins derived from the CLM4.0 LSM (Long et al., 2015; Wiese et al., 2016). GRACE ΔTWS is not a time-invariant measure (Wahr et al., 1998) and in the standard datasets all anomalies are given with respect to a baseline which is the mean over the period January 2004 to December 2009 (JPL NASA, 2019). Here, the completed available GRACE ΔTWS time series is examined with respect to climate anomalies in the same timeframe. Consequently, the JPL-Mascon ΔTWS dataset has been rescaled with respect to a time-mean taken over the whole period of GRACE operation (08.2002 – 07.2016), which is the study reference period (SRP) (JPL NASA, 2019).

As set out in Eq. (3), datasets for ΔSMS and ΔSWS derived from LSMs are required to determine ΔGWS from ΔTWS since observational data at the spatio-temporal scales of this study do not exist. Datasets for the 14 aquifer systems were drawn from NASA's Global Land Data Assimilation System (GLDAS) (Rodell et al., 2004) comprising the output from four different LSMs (Shamsudduha and Taylor, 2019): the Common [Community] Land Model (CLM, version 2.0), Noah (version 2.7.1), the Variable Infiltration Capacity (VIC) model (version 1.0), and Mosaic (version 1.0) (Rui and Beaudoing, 2019). As with ΔTWS, analysis of the four LSM datasets for ΔSWS+ΔSMS shows that their divergence summed over the entire time series is substantial, with a COV of 258%, suggesting that a LSM-ensemble mean approach may also not be appropriate for this analysis. Further, the inter- and intra- model variability of ΔSWS in the LSM datasets , assessed as surface runoff (e.g. Shamsudduha and Taylor, 2019; Thomas et al., 2017), is much less significant than that of ΔSMS (inter-model COV 378%). In the absence of consideration of ΔSWS, groundwater recharge is primarily determined by the effect of evapotranspiration on moisture in the soil zone (Long and Mahler, 2013). Therefore, for this study, modelling of ΔSMS is a key determinant of the outcomes for ΔGWS computed using Eq. (3) (de Vries and Simmers, 2002). Modelled soil profiles vary substantially in each of the 4 LSMs ranging in depth from 3.5m (Mosaic) to 1.9m (VIC) and, in vertical layers, from 10 (CLM) to 3 (VIC & Mosaic) (Rodell et al., 2004). CLM 2.0 (Bonan et al., 2002; Dai et al.,

https://doi.org/10.5194/esd-2019-83
Preprint. Discussion started: 16 January 2020


Earth System Dynamics
Discussions
Open Access
EGU

2003) with 3.4m depth and 10 vertical layers features the most well developed soil model (Scanlon et al., 2018), has been shown to perform well in comparative testing (Scanlon et al., 2018; Spennemann et al., 2014). In addition, CLM has demonstrated appropriate variability in initial ensemble model runs undertaken here, meaning that ΔSMS is almost always less than the magnitude of ΔTWS thereby ensuring that ΔGWS estimates derived from Eq. (3) are not arbitrarily high or low (Shamsudduha and Taylor, 2019). Therefore, this study employs a single model, CLM, for ΔSMS and ΔSWS rather than adopting a LSM ensemble mean approach.

2.2. *Climatology:*

Individual aquifer system shapefiles from the WHYMAP LASW were prepared as ASCII files and uploaded to KNMI Climate Explorer (KNMI Climate Explorer, 2018). This allowed a range of climate data to be extracted for the precise spatial boundaries of each system. In particular, precipitation (PCP) data from the CRU TS4.03 dataset at 0.5º resolution (Climate Research Unit, University of East Anglia, 2019) was obtained together with anomalies (PCPA) normalised for the SRP (2002-16). The CRU TS4.03 datasets together with the ΔGWS derived from JPL-Mascon ΔTWS and CLM 2.0 ΔSMS & ΔSWS, in accordance with Eq. (3), were used to create time series analyses to explore correlations over different time and volume components through integration. In this respect the use of 'annual' in this study implies the appropriate hydrological year.

In order to calibrate the time series for each aquifer system prior to further analysis, the lag between monthly PCP, as the primary climate-groundwater index, and monthly GRACE ΔTWS was set by maximising the Pearson Correlation Coefficient (PCC) between the two datasets, validated by point-wise verification of alignment of the time series. In the majority of cases, this comparison showed ΔTWS lagging PCP by two months. The lag for the PCPA time series were set in the same way with relation to ΔGWS but with the already determined PCP time series lag set as a minimum. In the case of all aquifer systems except for the Congo, Canning and Indus River Basins, this procedure resulted in a consistent lag being applied to all of the time series investigations of each aquifer. Initial investigations also established that only relatively weak first-order correlations exist between ΔTWS and other monthly observational climate data such as the self-calibrating Palmer Drought Severity Index (PDSI-sc) (Wells et al., 2004) and Mean Temperature anomalies (CPC GHCN/CAMS t2m analysis) (Fan and van den Dool, 2008). By comparison with both these measures, it appeared that PCPA carried a stronger climate variability signal due to the tropical/sub-tropical location of the selected aquifers (Allan et al., 2010; Shepherd, 2014). An analysis was then conducted to test for correlations between ΔGWS and a series of measures of precipitation. Three separate time series of

https://doi.org/10.5194/esd-2019-83
Preprint. Discussion started: 16 January 2020

precipitation were developed to examine the temporal response of the study LASW with respect to the process by which precipitation at the land surface contributes to ΔGWS:

1. PCP = monthly precipitation
2. PCPA = monthly precipitation anomalies with respect to the time-mean baseline for the study reference period (SRP – 2002-16)
3. ∫PCPA = cumulative monthly rainfall anomalies derived by integrating the PCPA time series

These monthly series were also summed to provide annual time series for each aquifer system. Correlation was measured using the PCC with statistical significance determined by a t-test with α=0.05 (Spearman, 1904). In addition, as previously stated, the CGIAR-CSI Global-Aridity dataset (Trabucco and Zomer, 2019) was obtained and a numerical AI for each aquifer was extracted as a spatial mean value using QGIS. AI was used to place each aquifer into the climate zone classification specified by the dataset as set out in Table 1. Of the climate zones relating to the 14 aquifer systems, 3 are Arid, 5 are Semi-Arid, 1 is Dry Semi-Humid, giving 9 in total in dryland zones (Corvalán et al., 2005), and 5 are Humid.

2.3. *Hydraulic Memory (HM):*

In using cumulative rainfall anomalies, this study invokes the concept of system memory (Weber and Stewart, 2004). Several studies have considered the question of hydraulic or hydrologic memory, both as it impacts soil moisture including land/atmosphere dynamics (Castro et al., 2009; Lo and Famiglietti, 2010; Wu et al., 2002), and groundwater (Currell et al., 2016; Cuthbert et al., 2019a; Güntner et al., 2007; Rodell and Famiglietti, 2001). Central to the definition of this 'memory' is that it represents the time taken for a system to re-equilibrate following a change in boundary conditions (Downing et al., 1974). In the case of an aquifer system, approximated to a one-dimensional flow of uniform diffusivity, the groundwater response time (GRT) is given by Eq. (4):

$$GRT = L^2 S/\beta T \quad (4)$$

where L is a measure of the scale of the system, S is the storativity, β is a dimensionless constant and T is transmissivity. Qualitatively Eq. (4) implies that long response times are characterised by large-scale systems and/or low hydraulic diffusivity (i.e. combination of high S and low T) (e.g. Kooi and Groen, 2003). An alternative approach to quantifying memory may be needed in more complex -

https://doi.org/10.5194/esd-2019-83
Preprint. Discussion started: 16 January 2020

Earth System Dynamics Discussions

and realistic – multidimensional flow situations (see Cuthbert et al., 2019a). Nevertheless, Eq. (4) still provides a useful order of magnitude approximation. Here, it is helpful to consider the response time as a delay between system input and system output whereby the output state *H*, at time *t*, is given by:

$$H(t) = \int_{-\infty}^{t} p(\tau)\, \theta(t-\tau)\, d\tau \qquad (5)$$

where $p(\boldsymbol{\tau})$ is the input state or function at time $\boldsymbol{\tau}$, $(t\text{-}\boldsymbol{\tau})$ is the delay between output and input, and $\boldsymbol{\theta}$ is an Impulse Response Function (IRF), also known as a transfer function (Long and Mahler, 2013). The IRF is a multi-parameter function that is intended to model the properties of the system so that the output of the IRF determines the time, *t*, at which the state *H* is reached. The hydraulic memory is quantified by the length of time that the effect of the input persists in the system. As the IRF is commonly exponential, making the equilibrium state asymptotic, system memory can be defined as the time interval at which the IRF is 95% complete. This approach has been successfully applied to modelling aquifer responses to precipitation validated by piezometry in both the USA (Long and Mahler, 2013) and the Netherlands (von Asmuth and Knotters, 2004). Alternatively, system memory may be defined as the length of time taken for the effect of the anomalous input to decay to 1/e of its starting value where this can be explicitly measured (Cuthbert et al., 2019a; Lo and Famiglietti, 2010). In relation to Eq. (5), chosen precipitation measures are $p(\boldsymbol{\tau})$ input functions, and ΔGWS represents *H(t)*, the output measure. The timestep, $\boldsymbol{\tau}$, for each of the precipitation time series used is as shown in Table 2. Correlation between ΔGWS (output) and a particular precipitation dataset (input) can be considered to be a measure of the persistence of the effect of that input integrated over the timestep. The degree of correlation between ΔGWS and annual ∫PCPA is thus indicative of the duration of HM in the aquifer system.

Time series:	**Timestep $\boldsymbol{\tau}$:**
PCP & PCPA	1 month
PCPA (HY)	1 year
∫PCPA (HY)	1 year$\leq\boldsymbol{\tau}\leq$14 years (*upper limit set by length of dataset*)

Table 2: The timestep, $\boldsymbol{\tau}$, for each of the precipitation time series investigated in the study

https://doi.org/10.5194/esd-2019-83
Preprint. Discussion started: 16 January 2020


Earth System Dynamics Discussions

***2.4.** Regional-Scale Hydrogeology:*

In an exploration of climate-groundwater dynamics using GRACE data, the lack of direct physical observational data means that it is necessary to demonstrate that results are not simply artefacts of modelling and signal processing (Rodell et al., 2009). The role of hydrogeology in determining groundwater dynamics is widely acknowledged (Befus et al., 2017; Cuthbert et al., 2019a; de Vries and Simmers, 2002; Lanen et al., 2013). Here, we seek to validate results inferred from GRACE data with reference to the physical characteristics of specific aquifer systems. In order to categorise the hydrogeology of each aquifer system, a number of available global datasets were sourced as raster files and interrogated in QGIS using the aquifer vector files from WHYMAP LASW. Examined datasets include:

1. Groundwater Response Time (GRT) (Cuthbert et al., 2019a)
2. Hydraulic Conductivity (K) and Porosity (Φ) GHLYMPS high resolution maps (Gleeson et al., 2014)
3. Water Table Depth (WTD) (Fan et al., 2013)

As defined above, the GRT is a temporal measure of the latency of aquifer systems that is derived from their scale and physical properties via Eq. (4). This measures relies on the other datasets listed for its calculation (Cuthbert et al., 2019a). K and Φ are high-resolution datasets derived from recently developed lithological maps of the Earth's surface (Hartmann and Moosdorf, 2012) and their computation uses established geological parameters (Gleeson et al., 2014). However, K is based on permeability mapping from hydrolithologies that have a standard deviation of ~2 orders of magnitude (Gleeson et al., 2011). WTD is 30 arc-second (~1km.) resolution dataset compiled from available observational data extended by modelled interpolation (Fan et al., 2013). All of these datasets are global and derived from combinations of observations and modelled data.

3.0. Results:

The main results for each aquifer system are given as a monthly time series of ΔTWS and ΔGWS vs. PCP and an annual time series of ΔGWS vs. PCPA and ∫PCPA, shown as **Figure 2 a-r** for dryland systems and **Figure 3 a-j** for humid systems. The outcomes are summarised in **Table 3**. As a general

https://doi.org/10.5194/esd-2019-83
Preprint. Discussion started: 16 January 2020

Earth System Dynamics Discussions
Open Access
EGU

result, all time series plots show a qualitative relationship between ΔGWS and PCP that exhibits interesting and potentially important spatio-temporal variations. The quantitative results show that for ΔGWS there is a strong correlation with annual ∫PCPA for aquifer systems in dryland environments whereas in humid environments, the strongest correlation is with monthly PCP. Three aquifers – Guarani Aquifer, Indus River Basin and Canning Basin - do not follow this general classification and anomalies are discussed further in section 4.3 below, and in the SI.

Aquifer System	**Monthly PCP vs ΔTWS**	**Monthly PCP vs ΔGWS**	**Monthly PCPA vs ΔGWS**	**Annual PCPA vs ΔGWS**	**Monthly ∫PCPA vs ΔGWS**	**Annual ∫PCPA vs ΔGWS**	**Aridity Class**	**Aridity Index**	**GWS Net Change over SRP**
Upper Kalahari	0.64 (2)	0.47 (2)	0.13 (2)	*0.22* (2)	0.67 (2)	**0.88** (2)	Semi-Arid	0.42	Increasing
Karoo	0.15 (7)	0.25 (7)	*0.07* (7)	*0.21* (7)	0.71 (7)	**0.88** (7)	Semi-Arid	0.28	Increasing
Senegal	0.67 (2)	0.55 (2)	0.15 (2)	*0.14* (2)	0.61 (2)	**0.87** (2)	Semi-Arid	0.20	Increasing
California Central Valley	0.53 (2)	0.46 (2)	0.26 (2)	0.56 (2)	0.60 (2)	**0.84** (2)	Semi-Arid	0.22	Decreasing
Great Artesian	0.45 (2)	0.33 (2)	0.34 (2)	0.67 (2)	0.61 (2)	**0.80** (2)	Arid	0.18	Stable
North China Plains	0.34 (2)	0.22 (2)	0.18 (2)	*0.26* (2)	0.65 (2)	**0.80** (2)	Dry Sub-Humid	0.57	Decreasing
Umm Ruwaba	0.87 (2)	**0.83** (2)	*0.12* (2)	0.55 (2)	0.20 (2)	0.64 (2)	Semi-Arid	0.33	Stable
Congo	0.67 (2)	**0.67** (2)	*0.11* (3)	0.43 (3)	0.27 (3)	0.62 (3)	Humid	1.22	Stable
Maranhao	0.82 (2)	**0.75** (2)	0.30 (2)	0.74 (2)	*0.11* (2)	0.40 (2)	Humid	0.91	Decreasing
Indus River	0.30 (1)	0.11 (1)	0.19 (3)	**0.37** (3)	0.15 (3)	*0.34* (3)	Arid	0.16	Decreasing
Amazon	0.88 (2)	**0.82** (2)	*0.08* (2)	*-0.12* (2)	0.13 (2)	*0.33* (2)	Humid	1.99	Stable
Guarani	0.50 (3)	0.48 (3)	0.42 (3)	**0.78** (3)	*0.01* (3)	*0.26* (3)	Humid	0.90	Increasing
Ganges-Brahmaputra	0.75 (2)	**0.69** (2)	0.06 (2)	0.03 (2)	0.03 (2)	*0.01* (2)	Humid	0.86	Decreasing
Canning	0.35 (2)	0.19 (2)	0.15 (3)	***0.26*** (3)	-0.15 (3)	*-0.01* (3)	Arid	0.13	Decreasing
Indus River post '08	0.42 (1)	0.15 (1)	0.21 (3)	0.73 (3)	0.34 (3)	0.89 (3)	Arid	0.16	Decreasing
Canning post '06	0.41 (2)	0.24 (2)	0.22 (3)	0.61 (3)	*-0.02* (3)	*0.24* (3)	Arid	0.13	Decreasing

Table 3: Summary Table of Results from Monthly & Annual Time Series & Aridity Datasets. Summary of all correlation results from time series datasets [Pearson Correlation Coefficient & (lag in months)] and the aridity indices derived from the CGIAR-CSI Global-Aridity dataset (Trabucco and Zomer, 2019). ΔGWS trend over SRP also shown. Results in italics fall below the t-test threshold. Aquifers are ranked in order of Pearson Correlation Coefficient for Annual ∫PCPA vs ΔGWS. For each Aquifer system the strongest ΔGWS correlation with PCP or PCPA is shown in bold. Truncated time series results shown for 2 systems.

https://doi.org/10.5194/esd-2019-83
Preprint. Discussion started: 16 January 2020

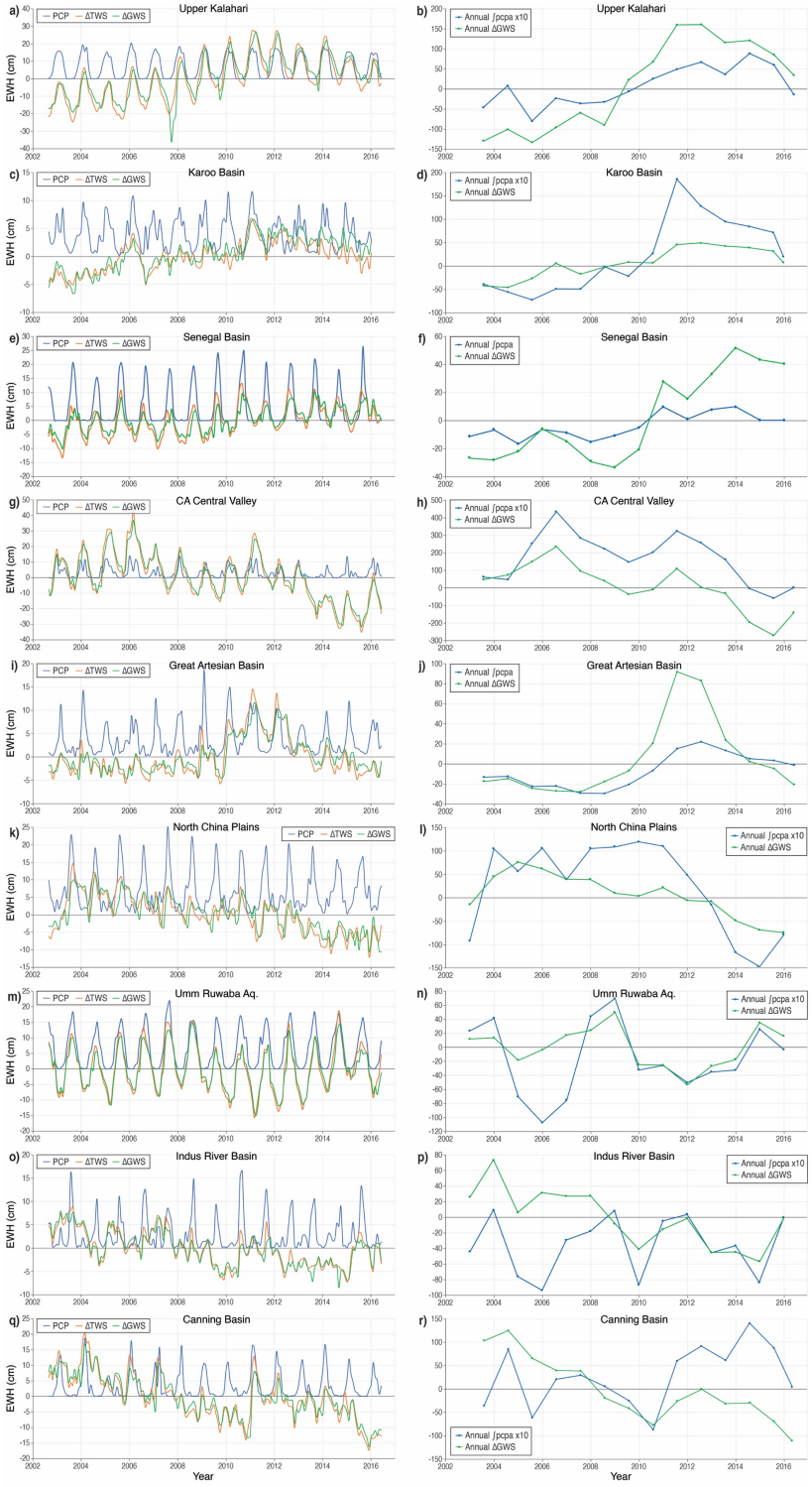

https://doi.org/10.5194/esd-2019-83
Preprint. Discussion started: 16 January 2020

Earth System Dynamics
Discussions
Open Access
EGU

Figure 2: Monthly ΔTWS & ΔGWS vs PCP and Annual ΔGWS vs ∫PCPA Time Series for each of the dryland climate zone aquifer systems, as labelled. Systems are ordered by decreasing PCC for annual ΔGWS vs ∫PCPA. All time series are plotted to the aquifer system lag as set out in Table 3, where ΔTWS (ΔGWS) lags PCP (PCPA) by the specified number of months. Y-axis units are Equivalent Water Height (EWH) in cm. Note the variation in the y-axis scales. 7 of the annual ∫PCPA data series have been scaled x10 for clarity, where indicated.

Figure 3: Monthly ΔTWS & ΔGWS vs PCP and Annual ΔGWS vs ∫PCPA Time Series for each of the humid climate zone aquifer systems, as labelled. Systems are ordered by decreasing PCC for annual ΔGWS vs ∫PCPA. All time series are plotted to the aquifer system lag as set out in Table 3, where ΔTWS lags PCP by the specified number of months. Y-axis units are Equivalent Water Height (EWH) in cm. Note the variation in the y-axis scales. Congo Basin annual ∫PCPA data series has been scaled x10 for clarity.

https://doi.org/10.5194/esd-2019-83
Preprint. Discussion started: 16 January 2020


Earth System Dynamics Discussions
Open Access
EGU

GRT, shown in **Figure 4**, is a measure of the time it takes for an aquifer system to equilibrate after a change in boundary conditions, as discussed above. For the 14 studied aquifers, it extends from centennial to millennial timescales as indicated from median values reported in **Tables 4 and S1**. For humid aquifers, GRT ranges from 100 to 350 years whereas for dryland systems GRT then escalates to values well in excess of 1,000 years for semi-arid and arid basins; the sub-humid North China Plains Aquifer has a GRT of ~550 years. This order of magnitude point of transition can be identified as the threshold between sensitive (rapid) and insensitive (slow) aquifer response times (Cuthbert et al., 2019a), which show a broad global relationship with aridity. This observation helps to explain groundwater storage responses to climate variability through the memory of the aquifer system defined by both physical characteristics and geographical location. The role of HM is discussed further in section 4.1.

Aquifer System	**Aridity Classification**	**Aridity Index**	**Annual ∫PCPA vs ΔGWS** ***[PCC] (lag in months)***	**GRT:** ***log (GRT) (GRT in yrs)***
Indus River post '08	Arid	0.16	0.89 (3)	3.96
Upper Kalahari	Semi-Arid	0.42	0.88 (2)	2.95
Karoo	Semi-Arid	0.28	0.88 (7)	5.74
Senegal	Semi-Arid	0.20	0.87 (2)	5.70
California Central Valley	Semi-Arid	0.22	0.84 (2)	3.01
Great Artesian	Arid	0.18	0.80 (2)	6.33
North China Plains	Dry Sub-Humid	0.57	0.80 (2)	2.74
Umm Ruwaba	Semi-Arid	0.33	0.64 (2)	4.42
Congo	Humid	1.22	0.62 (3)	2.12
Maranhao	Humid	0.91	0.40 (2)	2.55
Indus River	Arid	0.16	*0.34* (3)	3.96
Amazon	Humid	1.99	*0.33* (2)	2.03
Guarani	Humid	0.90	*0.26* (3)	2.20
Ganges-Brahmaputra	Humid	0.86	*0.01* (2)	2.10
Canning	Arid	0.13	*-0.01* (3)	6.46

Table 4: Relationship between Aridity Index, Climate and Regional-Scale Hydrogeology: Data linking climate and regional-scale hydrogeology to GW dynamics. *(Italicised results fall below t-test threshold.)*

https://doi.org/10.5194/esd-2019-83
Preprint. Discussion started: 16 January 2020

Earth System Dynamics
Discussions
Open Access
EGU

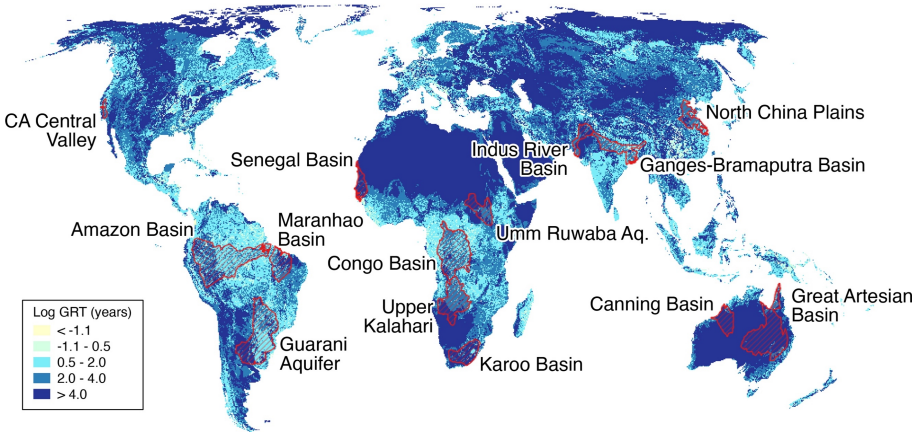

385

Figure 4: 14 of the World's Large-scale Aquifers (the Study Aquifers) overlaid on the GRT dataset [*original dataset from: (Cuthbert et al., 2019a)*]

390 Presented results represent the outcome of a detailed analysis of the available datasets and, as such, contain important assumptions that need to be acknowledged here. Firstly, the allocation of lag time has been done on a 'best-fit to the ΔTWS data' basis. It is therefore not derived from analysis of intrinsic physical characteristics of the aquifer systems but is consistent with the range of theoretical values derived from hydrodynamic first principles that anticipate a maximum lag time of
395 3 months for systems with a large GRT (Townley, 1995), as has been observed by Ahmed et al. (2011). Time lags have been tested for consistency through alignment of specific events in the various time series (Storch and Zwiers, 2001). The evident anomaly of a 7-month lag time for the Karoo Basin is discussed in the SI. Secondly, the restricted duration of the GRACE dataset should be acknowledged, particularly with regard to the annual time series. In mitigation, statistical
400 significance appears to be robust when tested (Zwiers and von Storch, 1995) and the use of PCPA and ∫PCPA datasets is designed to minimise the effect of seasonal climate and short-term trends in ΔGWS (Craddock, 1965). Thirdly, the use of Eq. (3) to derive ΔGWS from GRACE ΔTWS data represents a temporal and spatial approximation in representing sub-surface hydrological processes. Simply put, all water below the soil zone neither necessarily comprises GWS nor will it all eventually
405 reach GWS due to lateral flow processes. However, on the scale of the aquifer systems considered here, the use of Eq. (3) is a reasonable approximation (de Vries and Simmers, 2002).

https://doi.org/10.5194/esd-2019-83
Preprint. Discussion started: 16 January 2020


Earth System Dynamics Discussions

410

4.0. Discussion:

4.1. *Role of Hydraulic Memory (HM):*

415 A key finding of this study is that GRACE-derived ΔGWS correlates most strongly with annual ∫PCPA for large-scale aquifers in dryland environments of the tropics and sub-tropics whereas GRACE-derived ΔGWS correlates most strongly with monthly PCP in humid environments at these latitudes. Further, we show that there is correspondence between the annual ∫PCPA vs ΔGWS correlations and GRTs of large-scale aquifer systems (**Table 4**); the latter is a measure derived in accordance with Eq. 420 (4) (Cuthbert et al., 2019a). HM ultimately derives from the physical properties of the saturated portion of the aquifer system (Townley, 1995) and system memory as measured by Eq. (5) is representative of the physical properties of an aquifer system and its climate. Long and Mahler (2013), for example, used a total of 16 metrics to describe particular North American Karst aquifer systems in their IRF (***θ*** in Eq. (5)). In contrast, von Asmuth and Knotters (2004) used 4 parameters to 425 describe groundwater dynamics in their transfer function that they argue represents a more accurate description of the physical system than previously used parametric methods. Further, their description of groundwater dynamics is capable of accommodating non-stationary elements such as climate change and groundwater abstraction (von Asmuth and Knotters, 2004). HM as measured by Eq. (5) is therefore representative of both spatial and temporal variability in aquifer systems but HM 430 itself can vary spatio-temporally. Indeed the response time to a given boundary change can vary according to the physical circumstances, with persistence lasting from months to hundreds of thousands of years (Cuthbert et al., 2019a).

In this study, the GRACE dataset is not long enough to allow detailed IRF modelling of aquifer systems based on ΔGWS data, which would require an observational record longer than the 435 system memory (Long and Mahler, 2013). An extended GRACE series together with reduced uncertainty in the permeability dataset from which GRT is derived, may generate closer numerical matches between GRT (Eq. (4)) and HM as measured by the method of this study (Eq. (5)). Nevertheless, we show that aquifer responses to anomalous precipitation, discussed below, exhibit long HM in dryland environments and relatively short HM in humid environments. The 440 correspondence with GRT extends the classification to two broad categories: dryland environment/long HM/slow GRT and humid environment/short HM/rapid GRT. Note that these categories represent a simplification of the correspondence between HM derived from the study datasets and GRT, which in fact exhibits a spectrum in which Umm Ruwaba (dryland), Congo Basin

https://doi.org/10.5194/esd-2019-83
Preprint. Discussion started: 16 January 2020


Earth System Dynamics Discussions

and Maranhao (both humid) occupy an intermediate position in terms of the correlation between ΔGWS and annual ∫PCPA, as can be seen from **Table 3**. Aquifers in humid environments, with exception of the Congo Basin, generally exhibit less HM in this study than expected from GRT values. These humid aquifers, as can be seen from **Figure 4**, have some of their area with GRTs in the order of years to tens of years, perhaps meaning that a disproportionate amount of groundwater processes may be moving through these lower GRT areas. This may explain why humid regions have less HM overall than is implied by their median GRT.

4.2 *Aquifer Responses to Anomalous Precipitation:*

The annual time series of ΔGWS vs ∫PCPA for each aquifer have been examined to identify years in which the maximum annual increase in ΔGWS occurred, as identified by the steepest positive gradient of the ΔGWS line (**Table 5**). These years of extreme recharge, inferred from the increase in ΔGWS, are then further categorised by whether: (1) prior to the event ∫PCPA is negative, indicating anomalously dry conditions when soil moisture deficits (SMD) are likely to be widespread; and (2) the ∫PCPA is concurrently shifting from a negative to positive cumulative anomaly, associated with an extreme rainfall event. Finally, the NINO3.4 index for 2002-2016 (Huang et al., 2015) has been examined (KNMI Climate Explorer, 2018) to indicate the state of ENSO, the dominant control on equatorial precipitation, at the time of the recharge. Nearly all recharge events in dryland aquifer systems take place at a time of negative ∫PCPA (likely SMD), with most coinciding with extreme rainfall as recently observed in a pan-African study by Cuthbert et al., (2019b). Extreme recharge events also generally coincide with El Niño/La Niña events indicating an association with large-scale modes of climate variability identified previously in tropical Africa (Kolusu et al., 2019; Taylor et al., 2013b). In contrast, extreme recharge in humid aquifer systems is consistently associated with neither negative ∫PCPA (likely SMD), nor anomalous rainfall, though the latter is correlated with ENSO state.

https://doi.org/10.5194/esd-2019-83
Preprint. Discussion started: 16 January 2020

Earth System Dynamics Discussions
Open Access
EGU

480

Aquifer Systems grouped by AI: Dry	Year of Extreme Recharge	Negative ʃPCPA (likely SMD) [Y/N]	ʃPCPA Phase Change [Y/N]	ENSO State
Senegal	2010	Y	Y	La Nina
Umm Ruwaba	2014	Y	Y	Neutral
U. Kalahari	2008/9	Y	N	La Nina
Karoo	2010/11	N	N	La Nina
California CV	2015/16	Y	Y	El Nino
Indus River	2003	Y	Y	El Nino
Indus River	2015	Y	Y	El Nino
Great Artesian	2010/11	Y	Y	La Nina
Canning	2010/11	Y	Y	La Nina
North China Plains	2003	Y	Y	El Nino
Aquifer Systems by AI: Humid				
Ganges	2003	N	N	El Nino
Ganges	2011	Y	Y	Neutral
Amazon	2008/9	N	N	La Nina
Amazon	2011/12	N	N	La Nina
Maranhao	2008/9	N	N	La Nina
Guarani	2009/10	Y	N	El Nino
Guarani	2015/16	Y	Y	El Nino
Congo	2012/13	Y	N	Neutral

Table 5: Aquifer systems grouped by AI – Dry (Upper) and Humid (Lower). Extreme recharge years identified from annual time series by slope of ΔGWS plotted line. SMD status inferred by prior negative ʃPCPA and annual ʃPCPA phase change also derived from the same time series. ENSO state
485 from NINO3.4 Index (Huang et al., 2015).

4.3 *Anomalous Trends in Groundwater Storage:*

490 Over the SRP determined by the availability of GRACE data, six aquifer systems show a net decline in groundwater storage: California Central Valley, North China Plains, Maranhao, Ganges, Indus & Canning Basins. Of these, two aquifer systems (Indus River and Canning Basins) do not show a strong correlation between ΔGWS and any of the precipitation data series. **Table 4** shows that these same two aquifers do not fit the general classification of the 14 aquifer systems into either

https://doi.org/10.5194/esd-2019-83
Preprint. Discussion started: 16 January 2020

dryland/slow GRT/long HM or humid/rapid GRT/short HM systems. These anomalous characteristics may reflect groundwater storage decline through the escalation of groundwater abstraction referenced previously (Wada et al., 2014) and this hypothesis was tested through further analysis as follows below and in further detail in the SI.

The Indus River and Canning Basins superficially present similar stories of groundwater storage decline yet contextual analysis of their respective GRACE/CLM ΔGWS datasets reveals two quite different realities. The Indus River Basin supports a population of ~210 million people (Immerzeel et al., 2010) and its hydrology is strongly influenced by water supply from upstream of the basin, much of it intended for irrigation (Immerzeel et al., 2010). Surface water is augmented by groundwater abstraction, which supplies ~31% of the total irrigation demand, but it has been estimated that ~84% of the groundwater abstracted returns to the aquifer system as leakage from canals and intensively irrigated fields (Cheema et al., 2014). A net calculation of these effects on ΔGWS, which is detailed in the SI, shows that the underlying climate-groundwater dynamics are consistent with the GRT derived from the regional-scale hydrogeology of the aquifer system. In contrast, the Canning Basin is sparsely populated and is not a centre of agriculture (Richey et al., 2015). It is, however, a source of freshwater for iron-ore extraction in adjacent areas (Western Australia Department of Water, 2011) and very little of the abstracted groundwater is returned to the aquifer system as its use in mining causes it to become contaminated (Western Australia Department of Water, 2013). This contaminated groundwater is subsequently disposed in the sea or evaporation ponds (Prosser et al., 2011). The Canning Basin has a very slow GRT and, situated in an arid environment, is subject to low rates of groundwater recharge so that the physically sustainable rate of groundwater abstraction is expected to be very low (Scanlon et al., 2006). The analysis of the Indus and Canning Basins is evidence of how groundwater depletion, which has been reported elsewhere (e.g. Famiglietti, 2014; Rodell et al., 2009), impacts relationships between precipitation and ΔGWS.

***5.0 Conclusions**:*

Strong correlations are found between GRACE-derived annual ΔGWS and ∫PCPA for large-scale aquifer systems in dryland environments. This correlation is much weaker for large-scale aquifer systems in humid zones where a stronger correlation generally exists between monthly ΔGWS and monthly PCP. We propose that the correlation between annual ΔGWS and ∫PCPA demonstrates the existence of hydraulic memory which is central to large-scale climate-groundwater dynamics. For the studied aquifer systems, the measure of correlation between annual ΔGWS and ∫PCPA also shows

https://doi.org/10.5194/esd-2019-83
Preprint. Discussion started: 16 January 2020

very good correspondence with the groundwater response time, a measure of the hydraulic memory of an aquifer system derived from its regional-scale hydrogeological and catchment properties (Cuthbert et al., 2019a). The 14 aquifer systems can be broadly categorised into two groups, with each group listed in ascending order of groundwater response time:

- Group 1: Dryland/Long HM/slow GRT: North China Plains, Upper Kalahari, California Central Valley, Indus River, Umm Ruwaba, Senegal-Mauritanian, Karoo, Great Artesian & [Canning] Basins
- Group 2: Humid/Short HM/rapid GRT: Amazon, Ganges, Congo, Guarani, & Maranhao Basins

Aquifer systems in Group 1 may be less sensitive to seasonal climate variability but also vulnerable to long-term trends from which they will be slow to recover. In contrast, aquifers in Group 2 may be more sensitive to seasonal climate disturbances such as ENSO-related drought but may also be relatively quick to recover. These characteristics can be applied to anticipate the groundwater response to present conditions and to future pressures that can be expected from anthropogenic climate change (Taylor et al., 2013a). The results from the analysis of GRACE data are reconciled to regional-scale hydrogeological conditions, which gives confidence in their validity (Beven and Germann, 2013), albeit with the caveat regarding the uncertainties inherent in all the datasets used (Wilks, 2016).

The new GRACE follow on (GRACE-FO) project has now been launched (Frappart and Ramillien, 2018; Tapley et al., 2019), providing an opportunity to augment the existing GRACE ΔTWS dataset without recourse to modelling (Ahmed et al., 2019) and to give greater certainty in linking climate-groundwater dynamics to decadal and longer timescale climate systems including the Pacific Decadal Oscillation and Atlantic Multidecadal Oscillation (Wunsch, 1999). An extended dataset will improve the calibration of HM as it relates to specific aquifer systems, providing a robust context for monitoring ΔGWS, including groundwater decline, in real time and protecting fundamentally important groundwater resources.

Competing Interests: The authors declare no competing interests.

Authors' Contributions: SO led the analysis of datasets originally compiled by MS and MC, supplemented by datasets developed by SO; RT, CB and MS contributed to the original design of the study with key modifications made by SO; SO drafted the manuscript with input from RT; all authors contributed to, and commented on, revisions to the submitted manuscript.

https://doi.org/10.5194/esd-2019-83
Preprint. Discussion started: 16 January 2020

565 **References:**

Acker, J.G., Leptoukh, G., 2007. Online analysis enhances use of NASA Earth science data. Eos, Transactions American Geophysical Union 88, 14–17. https://doi.org/10.1029/2007EO020003

570 Ahmed, M., Sultan, M., Elbayoumi, T., Tissot, P., 2019. Forecasting GRACE Data over the African Watersheds Using Artificial Neural Networks. Remote Sensing 11, 1769. https://doi.org/10.3390/rs11151769

Allan, R.P., Soden, B.J., John, V.O., Ingram, W., Good, P., 2010. Current changes in tropical precipitation. Environ. Res. Lett. 5, 025205. https://doi.org/10.1088/1748-
575 9326/5/2/025205

Alley, W.M., Healy, R.W., LaBaugh, J.W., Reilly, T.E., 2002. Flow and Storage in Groundwater Systems. Science 296, 1985–1990. https://doi.org/10.1126/science.1067123

Becker, M., LLovel, W., Cazenave, A., Güntner, A., Crétaux, J.-F., 2010. Recent
580 hydrological behavior of the East African great lakes region inferred from GRACE, satellite altimetry and rainfall observations. Comptes Rendus Geoscience 342, 223–233. https://doi.org/10.1016/j.crte.2009.12.010

Befus, K.M., Jasechko, S., Luijendijk, E., Gleeson, T., Bayani Cardenas, M., 2017. The rapid yet uneven turnover of Earth's groundwater. Geophysical Research Letters 44, 5511–
585 5520. https://doi.org/10.1002/2017GL073322

Beven, K., Germann, P., 2013. Macropores and water flow in soils revisited: REVIEW. Water Resources Research 49, 3071–3092. https://doi.org/10.1002/wrcr.20156

BGR - WHYMAP - Large Aquifers [WWW Document], 2008. URL https://www.whymap.org/whymap/EN/Maps_Data/Additional_maps/whymap_largea
590 quifers_g.html (accessed 8.19.19).

Bierkens, M.F.P., 2015. Global hydrology 2015: State, trends, and directions: Global Hydrology 2015. Water Resources Research 51, 4923–4947. https://doi.org/10.1002/2015WR017173

Bonan, G.B., Oleson, K.W., Vertenstein, M., Levis, S., Zeng, X., Dai, Y., Dickinson, R.E.,
595 Yang, Z.-L., 2002. The Land Surface Climatology of the Community Land Model Coupled to the NCAR Community Climate Model. J. Climate 15, 3123–3149. https://doi.org/10.1175/1520-0442(2002)015<3123:TLSCOT>2.0.CO;2

Bonsor, H.C., Shamsudduha, M., Marchant, B.P., MacDonald, A.M., Taylor, R.G., 2018. Seasonal and Decadal Groundwater Changes in African Sedimentary Aquifers
600 Estimated Using GRACE Products and LSMs. Remote Sensing 10, 904. https://doi.org/10.3390/rs10060904

Castro, C.L., Beltrán-Przekurat, A.B., Pielke, R.A., 2009. Spatiotemporal Variability of Precipitation, Modeled Soil Moisture, and Vegetation Greenness in North America within the Recent Observational Record. J. Hydrometeor. 10, 1355–1378.
605 https://doi.org/10.1175/2009JHM1123.1

Cheema, M. j. m., Immerzeel, W. w., Bastiaanssen, W. g. m., 2014. Spatial Quantification of Groundwater Abstraction in the Irrigated Indus Basin. Groundwater 52, 25–36. https://doi.org/10.1111/gwat.12027

Chen, J.L., Wilson, C.R., Tapley, B.D., 2010. The 2009 exceptional Amazon flood and
610 interannual terrestrial water storage change observed by GRACE. Water Resources Research 46. https://doi.org/10.1029/2010WR009383

Chen, J.L., Wilson, C.R., Tapley, B.D., Scanlon, B., Güntner, A., 2016. Long-term groundwater storage change in Victoria, Australia from satellite gravity and in situ

https://doi.org/10.5194/esd-2019-83
Preprint. Discussion started: 16 January 2020

observations. Global and Planetary Change 139, 56–65. https://doi.org/10.1016/j.gloplacha.2016.01.002

Climate Research Unit, University of East Anglia, 2019. CRU TS Version 4.01 [WWW Document]. CRU TS Version 4.01. URL https://crudata.uea.ac.uk/cru/data/hrg/cru_ts_4.01/ (accessed 8.20.19).

Corvalán, C., Hales, S., McMichael, A.J., Millennium Ecosystem Assessment (Program), World Health Organization (Eds.), 2005. Ecosystems and human well-being: health synthesis, Millennium ecosystem assessment. World Health Organization, Geneva, Switzerland.

Craddock, J.M., 1965. The Analysis of Meteorological Time Series for Use in Forecasting. Journal of the Royal Statistical Society. Series D (The Statistician) 15, 167–190. https://doi.org/10.2307/2987390

Currell, M., Gleeson, T., Dahlhaus, P., 2016. A New Assessment Framework for Transience in Hydrogeological Systems. Groundwater 54, 4–14. https://doi.org/10.1111/gwat.12300

Cuthbert, M.O., Gleeson, T., Moosdorf, N., Befus, K.M., Schneider, A., Hartmann, J., Lehner, B., 2019a. Global patterns and dynamics of climate–groundwater interactions. Nature Climate Change 1. https://doi.org/10.1038/s41558-018-0386-4

Cuthbert, M.O., Taylor, R.G., Favreau, G., Todd, M.C., Shamsudduha, M., Villholth, K.G., MacDonald, A.M., Scanlon, B.R., Kotchoni, D.O.V., Vouillamoz, J.-M., Lawson, F.M.A., Adjomayi, P.A., Kashaigili, J., Seddon, D., Sorensen, J.P.R., Ebrahim, G.Y., Owor, M., Nyenje, P.M., Nazoumou, Y., Goni, I., Ousmane, B.I., Sibanda, T., Ascott, M.J., Macdonald, D.M.J., Agyekum, W., Koussoubé, Y., Wanke, H., Kim, H., Wada, Y., Lo, M.-H., Oki, T., Kukuric, N., 2019b. Observed controls on resilience of groundwater to climate variability in sub-Saharan Africa. Nature 572, 230–234. https://doi.org/10.1038/s41586-019-1441-7

Dai, Y., Zeng, X., Dickinson, R.E., Baker, I., Bonan, G.B., Bosilovich, M.G., Denning, A.S., Dirmeyer, P.A., Houser, P.R., Niu, G., Oleson, K.W., Schlosser, C.A., Yang, Z.-L., 2003. The Common Land Model. Bull. Amer. Meteor. Soc. 84, 1013–1024. https://doi.org/10.1175/BAMS-84-8-1013

Damkjaer, S., Taylor, R., 2017. The measurement of water scarcity: Defining a meaningful indicator. Ambio 46, 513–531. https://doi.org/10.1007/s13280-017-0912-z

de Vries, J.J., Simmers, I., 2002. Groundwater recharge: an overview of processes and challenges. Hydrogeology Journal 10, 5–17. https://doi.org/10.1007/s10040-001-0171-7

Döll, P., Douville, H., Güntner, A., Müller Schmied, H., Wada, Y., 2016. Modelling Freshwater Resources at the Global Scale: Challenges and Prospects. Surv Geophys 37, 195–221. https://doi.org/10.1007/s10712-015-9343-1

Döll, P., Hoffmann-Dobrev, H., Portmann, F.T., Siebert, S., Eicker, A., Rodell, M., Strassberg, G., Scanlon, B.R., 2012. Impact of water withdrawals from groundwater and surface water on continental water storage variations. Journal of Geodynamics, Mass Transport and Mass Distribution in the System Earth 59–60, 143–156. https://doi.org/10.1016/j.jog.2011.05.001

Döll, P., Müller Schmied, H., Schuh, C., Portmann, F.T., Eicker, A., 2014. Global-scale assessment of groundwater depletion and related groundwater abstractions: Combining hydrological modeling with information from well observations and GRACE satellites. Water Resources Research 50, 5698–5720. https://doi.org/10.1002/2014WR015595

https://doi.org/10.5194/esd-2019-83
Preprint. Discussion started: 16 January 2020

Downing, R.A., Oakes, D.B., Wilkinson, W.B., Wright, C.E., 1974. Regional development of groundwater resources in combination with surface water. Journal of Hydrology 22, 155–177. https://doi.org/10.1016/0022-1694(74)90102-4

Famiglietti, J.S., 2014. The global groundwater crisis. Nature Climate Change 4, 945–948. https://doi.org/10.1038/nclimate2425

Fan, Y., Li, H., Miguez-Macho, G., 2013. Global Patterns of Groundwater Table Depth. Science 339, 940–943. https://doi.org/10.1126/science.1229881

Fan, Y., van den Dool, H., 2008. A global monthly land surface air temperature analysis for 1948–present. Journal of Geophysical Research: Atmospheres 113. https://doi.org/10.1029/2007JD008470

Frappart, F., Ramillien, G., 2018. Monitoring Groundwater Storage Changes Using the Gravity Recovery and Climate Experiment (GRACE) Satellite Mission: A Review. Remote Sensing 10, 829. https://doi.org/10.3390/rs10060829

Getirana, A., Kumar, S., Girotto, M., Rodell, M., 2017. Rivers and Floodplains as Key Components of Global Terrestrial Water Storage Variability. Geophysical Research Letters 44, 10,359-10,368. https://doi.org/10.1002/2017GL074684

Gleeson, T., Moosdorf, N., Hartmann, J., van Beek, L.P.H., 2014. A glimpse beneath earth's surface: GLobal HYdrogeology MaPS (GLHYMPS) of permeability and porosity. Geophysical Research Letters 41, 3891–3898. https://doi.org/10.1002/2014GL059856

Gleeson, T., Smith, L., Moosdorf, N., Hartmann, J., Dürr, H.H., Manning, A.H., Beek, L.P.H. van, Jellinek, A.M., 2011. Mapping permeability over the surface of the Earth. Geophysical Research Letters 38. https://doi.org/10.1029/2010GL045565

Graaf, I.E.M. de, Gleeson, T., Beek, L.P.H. (Rens) van, Sutanudjaja, E.H., Bierkens, M.F.P., 2019. Environmental flow limits to global groundwater pumping. Nature 574, 90–94. https://doi.org/10.1038/s41586-019-1594-4

Güntner, A., Stuck, J., Werth, S., Döll, P., Verzano, K., Merz, B., 2007. A global analysis of temporal and spatial variations in continental water storage. Water Resources Research 43. https://doi.org/10.1029/2006WR005247

Hartmann, J., Moosdorf, N., 2012. The new global lithological map database GLiM: A representation of rock properties at the Earth surface. Geochemistry, Geophysics, Geosystems 13. https://doi.org/10.1029/2012GC004370

Henry, C.M., Allen, D.M., Huang, J., 2011. Groundwater storage variability and annual recharge using well-hydrograph and GRACE satellite data. Hydrogeol J 19, 741–755. https://doi.org/10.1007/s10040-011-0724-3

Huang, B., Banzon, V.F., Freeman, E., Lawrimore, J., Liu, W., Peterson, T.C., Smith, T.M., Thorne, P.W., Woodruff, S.D., Zhang, H.-M., 2015. Extended Reconstructed Sea Surface Temperature (ERSST), Version 4. https://doi.org/10.7289/v5kd1vvf

Huang, Z., Pan, Y., Gong, H., Yeh, P.J.-F., Li, X., Zhou, D., Zhao, W., 2015. Subregional-scale groundwater depletion detected by GRACE for both shallow and deep aquifers in North China Plain. Geophysical Research Letters 42, 1791–1799. https://doi.org/10.1002/2014GL062498

Immerzeel, W.W., van Beek, L.P.H., Bierkens, M.F.P., 2010. Climate Change Will Affect the Asian Water Towers. Science 328, 1382–1385. https://doi.org/10.1126/science.1183188

JPL NASA, 2019. Frequently Asked Questions | About [WWW Document]. GRACE Tellus. URL https://grace.jpl.nasa.gov/about/faq (accessed 8.20.19).

KNMI Climate Explorer, 2018. Climate Explorer: Starting point [WWW Document]. KNMI Climate Explorer. URL https://climexp.knmi.nl/start.cgi?id=b08c094a879f19247ae5839cc6377977 (accessed 12.22.18).

https://doi.org/10.5194/esd-2019-83
Preprint. Discussion started: 16 January 2020

Kolusu, S.R., Shamsudduha, M., Todd, M.C., Taylor, R.G., Seddon, D., Kashaigili, J.J., Ebrahim, G.Y., Cuthbert, M.O., Sorensen, J.P.R., Villholth, K.G., MacDonald, A.M., MacLeod, D.A., 2019. The El Niño event of 2015–2016: climate anomalies and their impact on groundwater resources in East and Southern Africa. Hydrology and Earth System Sciences 23, 1751–1762. https://doi.org/10.5194/hess-23-1751-2019

Kooi, H., Groen, J., 2003. Geological processes and the management of groundwater resources in coastal areas. Netherlands Journal of Geosciences 82, 31–40. https://doi.org/10.1017/S0016774600022770

Landerer, F.W., 2019. Personal correspondence [WWW Document]. email. URL https://outlook.office.com/owa/?realm=acl.ac.uk&path=/attachmentlightbox (accessed 6.14.19).

Landerer, F.W., Swenson, S.C., 2012. Accuracy of scaled GRACE terrestrial water storage estimates. Water Resources Research 48. https://doi.org/10.1029/2011WR011453

Lanen, H.A.J. van, Wanders, N., Tallaksen, L.M., Loon, A.F. van, 2013. Hydrological drought across the world: impact of climate and physical catchment structure [WWW Document]. Hydrology and Earth System Sciences. http://dx.doi.org/10.5194/hess-17-1715-2013

Lo, M.-H., Famiglietti, J.S., 2010. Effect of water table dynamics on land surface hydrologic memory. Journal of Geophysical Research: Atmospheres 115. https://doi.org/10.1029/2010JD014191

Long, A.J., Mahler, B.J., 2013. Prediction, time variance, and classification of hydraulic response to recharge in two karst aquifers. Hydrology and Earth System Sciences 17, 281–294. https://doi.org/10.5194/hess-17-281-2013

Long, D., Longuevergne, L., Scanlon, B.R., 2015. Global analysis of approaches for deriving total water storage changes from GRACE satellites. Water Resources Research 51, 2574–2594. https://doi.org/10.1002/2014WR016853

Mémin, A., Flament, T., Alizier, B., Watson, C., Rémy, F., 2015. Interannual variation of the Antarctic Ice Sheet from a combined analysis of satellite gravimetry and altimetry data. Earth and Planetary Science Letters C, 150–156. https://doi.org/10.1016/j.epsl.2015.03.045

Ni, S., Chen, J., Wilson, C.R., Li, J., Hu, X., Fu, R., 2018. Global Terrestrial Water Storage Changes and Connections to ENSO Events. Surv Geophys 39, 1–22. https://doi.org/10.1007/s10712-017-9421-7

Overgaard, J., Rosbjerg, D., Butts, M.B., 2006. Land-surface modelling in hydrological perspective - a review. Biogeosciences 3, 229–241.

Phillips, T., Nerem, R.S., Fox-Kemper, B., Famiglietti, J.S., Rajagopalan, B., 2012. The influence of ENSO on global terrestrial water storage using GRACE. Geophysical Research Letters 39, n/a-n/a. https://doi.org/10.1029/2012GL052495

Prosser, I., Wolf, L., Littleboy, A., 2011. Water in mining and industry 12.

Ramillien, G., Frappart, F., Seoane, L., 2014. Application of the Regional Water Mass Variations from GRACE Satellite Gravimetry to Large-Scale Water Management in Africa. Remote Sensing 6, 7379–7405. https://doi.org/10.3390/rs6087379

Richey, A.S., Thomas, B.F., Lo, M.-H., Reager, J.T., Famiglietti, J.S., Voss, K., Swenson, S., Rodell, M., 2015. Quantifying renewable groundwater stress with GRACE. Water Resources Research 51, 5217–5238. https://doi.org/10.1002/2015WR017349

Rodell, M., Famiglietti, J.S., 2001. An analysis of terrestrial water storage variations in Illinois with implications for the Gravity Recovery and Climate Experiment (GRACE). Water Resources Research 37, 1327–1339. https://doi.org/10.1029/2000WR900306

https://doi.org/10.5194/esd-2019-83
Preprint. Discussion started: 16 January 2020

Rodell, M., Houser, P.R., Jambor, U., Gottschalck, J., Mitchell, K., Meng, C.-J., Arsenault, K., Cosgrove, B., Radakovich, J., Bosilovich, M., Entin, J.K., Walker, J.P., Lohmann, D., Toll, D., 2004. The Global Land Data Assimilation System. Bull. Amer. Meteor. Soc. 85, 381–394. https://doi.org/10.1175/BAMS-85-3-381

Rodell, M., Velicogna, I., Famiglietti, J.S., 2009. Satellite-based estimates of groundwater depletion in India. Nature 460, 999–1002. https://doi.org/10.1038/nature08238

Rui, H., Beaudoing, H., 2019. Global Land Data Assimilation System (GLDAS-1) Products README 32.

Sakumura, C., Bettadpur, S., Bruinsma, S., 2014. Ensemble prediction and intercomparison analysis of GRACE time-variable gravity field models. Geophysical Research Letters 41, 1389–1397. https://doi.org/10.1002/2013GL058632

Scanlon, B.R., Healy, R.W., Cook, P.G., 2002. Choosing appropriate techniques for quantifying groundwater recharge. Hydrogeology Journal 10, 18–39. https://doi.org/10.1007/s10040-001-0176-2

Scanlon, B.R., Keese, K.E., Flint, A.L., Flint, L.E., Gaye, C.B., Edmunds, W.M., Simmers, I., 2006. Global synthesis of groundwater recharge in semiarid and arid regions. Hydrological Processes 20, 3335–3370. https://doi.org/10.1002/hyp.6335

Scanlon, B.R., Zhang, Z., Save, H., Sun, A.Y., Schmied, H.M., Beek, L.P.H. van, Wiese, D.N., Wada, Y., Long, D., Reedy, R.C., Longuevergne, L., Döll, P., Bierkens, M.F.P., 2018. Global models underestimate large decadal declining and rising water storage trends relative to GRACE satellite data. PNAS 115, E1080–E1089. https://doi.org/10.1073/pnas.1704665115

Scanlon, B.R., Zhang, Z., Save, H., Wiese, D.N., Landerer, F.W., Long, D., Longuevergne, L., Chen, J., 2016. Global evaluation of new GRACE mascon products for hydrologic applications: GLOBAL ANALYSIS OF GRACE MASCON PRODUCTS. Water Resources Research 52, 9412–9429. https://doi.org/10.1002/2016WR019494

Shamsudduha, M., Taylor, R.G., 2019. Changes in global groundwater storage from GRACE: uncertainty and the role of extreme precipitation 85.

Shamsudduha, M., Taylor, R.G., Jones, D., Longuevergne, L., Owor, M., Tindimugaya, C., 2017. Recent changes in terrestrial water storage in the Upper Nile Basin: an evaluation of commonly used gridded GRACE products.

Shamsudduha, M., Taylor, R.G., Longuevergne, L., 2012. Monitoring groundwater storage changes in the highly seasonal humid tropics: Validation of GRACE measurements in the Bengal Basin. Water Resources Research 48. https://doi.org/10.1029/2011WR010993

Shepherd, T.G., 2014. Atmospheric circulation as a source of uncertainty in climate change projections. Nature Geoscience 7, 703–708. https://doi.org/10.1038/ngeo2253

Sood, A., Smakhtin, V., 2015. Global hydrological models: a review. Hydrological Sciences Journal 60, 549–565. https://doi.org/10.1080/02626667.2014.950580

Spearman, C., 1904. The Proof and Measurement of Association between Two Things. The American Journal of Psychology 15, 72–101. https://doi.org/10.2307/1412159

Spennemann, P.C., Rivera, J.A., Saulo, A.C., Penalba, O.C., 2014. A Comparison of GLDAS Soil Moisture Anomalies against Standardized Precipitation Index and Multisatellite Estimations over South America. J. Hydrometeor. 16, 158–171. https://doi.org/10.1175/JHM-D-13-0190.1

Storch, H. von, Zwiers, F.W., 2001. Statistical Analysis in Climate Research. Cambridge University Press.

Tapley, B.D., Bettadpur, S., Watkins, M., Reigber, C., 2004. The gravity recovery and climate experiment: Mission overview and early results. Geophysical Research Letters. https://doi.org/10.1029/2004GL019920@10.1002/(ISSN)1944-8007.GRL40

https://doi.org/10.5194/esd-2019-83
Preprint. Discussion started: 16 January 2020

Tapley, B.D., Watkins, M.M., Flechtner, F., Reigber, C., Bettadpur, S., Rodell, M., Sasgen, I., Famiglietti, J.S., Landerer, F.W., Chambers, D.P., Reager, J.T., Gardner, A.S., Save, H., Ivins, E.R., Swenson, S.C., Boening, C., Dahle, C., Wiese, D.N., Dobslaw, H., Tamisiea, M.E., Velicogna, I., 2019. Contributions of GRACE to understanding climate change. Nature Climate Change 9, 358. https://doi.org/10.1038/s41558-019-0456-2

Taylor, R.G., Koussis, A.D., Tindimugaya, C., 2009. Groundwater and climate in Africa—a review. Hydrological Sciences Journal 54, 655–664. https://doi.org/10.1623/hysj.54.4.655

Taylor, R.G., Scanlon, B., Döll, P., Rodell, M., van Beek, R., Wada, Y., Longuevergne, L., Leblanc, M., Famiglietti, J.S., Edmunds, M., Konikow, L., Green, T.R., Chen, J., Taniguchi, M., Bierkens, M.F.P., MacDonald, A., Fan, Y., Maxwell, R.M., Yechieli, Y., Gurdak, J.J., Allen, D.M., Shamsudduha, M., Hiscock, K., Yeh, P.J.-F., Holman, I., Treidel, H., 2013a. Ground water and climate change. Nature Climate Change 3, 322–329. https://doi.org/10.1038/nclimate1744

Taylor, R.G., Todd, M.C., Kongola, L., Maurice, L., Nahozya, E., Sanga, H., MacDonald, A.M., 2013b. Evidence of the dependence of groundwater resources on extreme rainfall in East Africa. Nature Climate Change 3, 374–378. https://doi.org/10.1038/nclimate1731

Thomas, B.F., Caineta, J., Nanteza, J., 2017. Global Assessment of Groundwater Sustainability Based On Storage Anomalies. Geophysical Research Letters 44, 11,445-11,455. https://doi.org/10.1002/2017GL076005

Tiwari, V.M., Wahr, J., Swenson, S., 2009. Dwindling groundwater resources in northern India, from satellite gravity observations. Geophysical Research Letters 36. https://doi.org/10.1029/2009GL039401

Townley, L.R., 1995. The response of aquifers to periodic forcing. Advances in Water Resources 18, 125–146. https://doi.org/10.1016/0309-1708(95)00008-7

Trabucco, A., Zomer, R., 2019. Global Aridity Index and Potential Evapotranspiration (ET0) Climate Database v2. https://doi.org/10.6084/m9.figshare.7504448.v3

Trenberth, K.E., 2011. Changes in precipitation with climate change. Climate Research 47, 123–138. https://doi.org/10.3354/cr00953

von Asmuth, J.R., Knotters, M., 2004. Characterising groundwater dynamics based on a system identification approach. Journal of Hydrology 296, 118–134. https://doi.org/10.1016/j.jhydrol.2004.03.015

Wada, Y., 2016. Modeling Groundwater Depletion at Regional and Global Scales: Present State and Future Prospects. Surveys in Geophysics 37, 419–451. https://doi.org/10.1007/s10712-015-9347-x

Wada, Y., Wisser, D., Bierkens, M.F.P., 2014. Global modeling of withdrawal, allocation and consumptive use of surface water and groundwater resources 27.

Wahr, J., Molenaar, M., Bryan, F., 1998. Time variability of the Earth's gravity field: Hydrological and oceanic effects and their possible detection using GRACE. Journal of Geophysical Research: Solid Earth 103, 30205–30229. https://doi.org/10.1029/98JB02844

Watkins, M.M., Wiese, D.N., Yuan, D.-N., Boening, C., Landerer, F.W., 2015. Improved methods for observing Earth's time variable mass distribution with GRACE using spherical cap mascons. Journal of Geophysical Research: Solid Earth 120, 2648–2671. https://doi.org/10.1002/2014JB011547

Weber, K., Stewart, M., 2004. A Critical Analysis of the Cumulative Rainfall Departure Concept. Ground Water; Dublin 42, 935–938.

https://doi.org/10.5194/esd-2019-83
Preprint. Discussion started: 16 January 2020

Wells, N., Goddard, S., Hayes, M.J., 2004. A Self-Calibrating Palmer Drought Severity Index. J. Climate 17, 2335–2351. https://doi.org/10.1175/1520-0442(2004)017<2335:ASPDSI>2.0.CO;2

Western Australia Department of Water, 2013. Western Australian water in mining guideline.

Western Australia Department of Water, 2011. Capacity of water resources in the Mid west to meet mining and industrial growth: a status report. Dept. of Water, Perth, W.A.

Wiese, D.N., Landerer, F.W., Watkins, M.M., 2016. Quantifying and reducing leakage errors in the JPL RL05M GRACE mascon solution. Water Resources Research 52, 7490–7502. https://doi.org/10.1002/2016WR019344

Wilks, D.S., 2016. "The Stippling Shows Statistically Significant Grid Points": How Research Results are Routinely Overstated and Overinterpreted, and What to Do about It. Bull. Amer. Meteor. Soc. 97, 2263–2273. https://doi.org/10.1175/BAMS-D-15-00267.1

Wood, E.F., Roundy, J.K., Troy, T.J., Beek, L.P.H. van, Bierkens, M.F.P., Blyth, E., Roo, A. de, Döll, P., Ek, M., Famiglietti, J., Gochis, D., Giesen, N. van de, Houser, P., Jaffé, P.R., Kollet, S., Lehner, B., Lettenmaier, D.P., Peters-Lidard, C., Sivapalan, M., Sheffield, J., Wade, A., Whitehead, P., 2011. Hyperresolution global land surface modeling: Meeting a grand challenge for monitoring Earth's terrestrial water. Water Resources Research 47. https://doi.org/10.1029/2010WR010090

Wu, W., Geller, M.A., Dickinson, R.E., 2002. The Response of Soil Moisture to Long-Term Variability of Precipitation. J. Hydrometeor. 3, 604–613. https://doi.org/10.1175/1525-7541(2002)003<0604:TROSMT>2.0.CO;2

Wunsch, C., 1999. The Interpretation of Short Climate Records, with Comments on the North Atlantic and Southern Oscillations. Bulletin of the American Meteorological Society 80, 245–255. https://doi.org/10.1175/1520-0477(1999)080<0245:TIOSCR>2.0.CO;2

Xavier, L., Becker, M., Cazenave, A., Longuevergne, L., Llovel, W., Filho, O.C.R., 2010. Interannual variability in water storage over 2003–2008 in the Amazon Basin from GRACE space gravimetry, in situ river level and precipitation data. Remote Sensing of Environment 114, 1629–1637. https://doi.org/10.1016/j.rse.2010.02.005

Xie, X., Xu, C., Wen, Y., Li, W., 2018. Monitoring Groundwater Storage Changes in the Loess Plateau Using GRACE Satellite Gravity Data, Hydrological Models and Coal Mining Data. Remote Sensing 10, 605. https://doi.org/10.3390/rs10040605

Yeh, P.J.-F., Swenson, S.C., Famiglietti, J.S., Rodell, M., 2006. Remote sensing of groundwater storage changes in Illinois using the Gravity Recovery and Climate Experiment (GRACE). Water Resources Research 42. https://doi.org/10.1029/2006WR005374

Zwiers, F.W., von Storch, H., 1995. Taking Serial Correlation into Account in Tests of the Mean. J. Climate 8, 336–351. https://doi.org/10.1175/1520-0442(1995)008<0336:TSCIAI>2.0.CO;2

Data Availability

Supplementary information is available for this paper as a single PDF file. Data generated and used in this study can be made available upon request to the corresponding author.